JACS
JOURNAL OF THE AMERICAN CHEMICAL SOCIETY

ARTICLE

pubs.acs.org/JACS

Electron- and Hydride-Transfer Reactivity of an Isolable Manganese(V)−Oxo Complex

Shunichi Fukuzumi,*[,†,‡] Hiroaki Kotani,[†] Katharine A. Prokop,[§] and David P. Goldberg*[,§]

[†]Department of Material and Life Science, Graduate School of Engineering, Osaka University, Suita, Osaka 565-0871, Japan

[‡]Department of Bioinspired Science, Ewha Womans University, Seoul 120-750, Korea

[§]Department of Chemistry, Johns Hopkins University, Baltimore, Maryland 21218, United States

Supporting Information

ABSTRACT: The electron-transfer and hydride-transfer properties of an isolated manganese(V)−oxo complex, $(TBP_8Cz)Mn^{V}(O)$ (**1**) (TBP_8Cz=octa-*tert*-butylphenylcorrolazinato) were determined by spectroscopic and kinetic methods. The manganese(V)−oxo complex **1** reacts rapidly with a series of ferrocene derivatives ($[Fe(C_5H_4Me)_2]$, $[Fe(C_5HMe_4)_2]$, and ($[Fe(C_5Me_5)_2]$ = Fc*) to give the direct formation of $[(TBP_8Cz)Mn^{III}(OH)]^-$ ($[$**2-OH**$]^-$), a two-electron-reduced product. The stoichiometry of these electron-transfer reactions was found to be (Fc derivative)/**1** = 2:1 by spectral titration. The rate constants of electron transfer from ferrocene derivatives to **1** at room temperature in benzonitrile were obtained, and the successful application of Marcus theory allowed for the determination of the reorganization energies (λ) of electron transfer. The λ values of electron transfer from the ferrocene derivatives to **1** are lower than those reported for a manganese(IV)−oxo porphyrin. The presumed one-electron-reduced intermediate, a Mn^{IV} complex, was not observed during the reduction of **1**. However, a Mn^{IV} complex was successfully generated via one-electron oxidation of the Mn^{III} precursor complex **2** to give $[(TBP_8Cz)Mn^{IV}]^+$ (**3**). Complex **3** exhibits a characteristic absorption band at λ_{max} = 722 nm and an EPR spectrum at 15 K with g'_{max} = 4.68, g'_{mid} = 3.28, and g'_{min} = 1.94, with well-resolved ^{55}Mn hyperfine coupling, indicative of a d^3 Mn^{IV} $S=^3/_2$ ground state. Although electron transfer from $[Fe(C_5H_4Me)_2]$ to **1** is endergonic (uphill), two-electron reduction of **1** is made possible in the presence of proton donors (e.g., CH_3CO_2H, CF_3CH_2OH, and CH_3OH). In the case of CH_3CO_2H, saturation behavior for the rate constants of electron transfer (k_{et}) versus acid concentration was observed, providing insight into the critical involvement of H^+ in the mechanism of electron transfer. Complex **1** was also shown to be competent to oxidize a series of dihydronicotinamide adenine dinucleotide (NADH) analogues via formal hydride transfer to produce the corresponding NAD^+ analogues and $[$**2-OH**$]^-$. The logarithms of the observed second-order rate constants of hydride transfer (k_H) from NADH analogues to **1** are linearly correlated with those of hydride transfer from the same series of NADH analogues to *p*-chloranil.

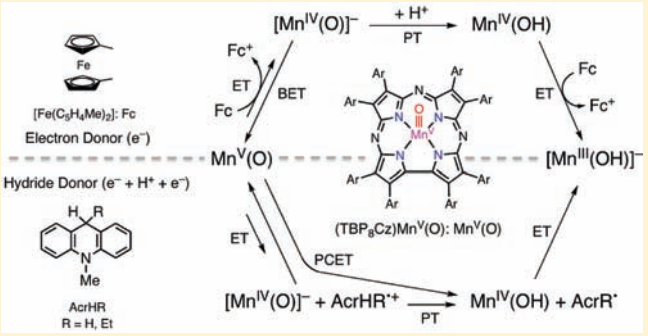

INTRODUCTION

High-valent metal−oxo species are frequently invoked as the key oxidizing intermediates in various oxidation reactions of heme and non-heme iron enzymes.[1,2] For example, the cytochrome P450 family of enzymes is believed to depend on the formation of a transient iron(IV)−oxo porphyrin π-radical cation, $[(Porp)^{\bullet+}Fe^{IV}(O)]^+$ (Porp = porphinato dianion), as the critical active oxidizing intermediate in the catalytic cycle.[3,4] Significant efforts have been expended in generating the corresponding manganese−oxo porphyrins $[(Porp)Mn^{V}(O)]^+$ and $(Porp)Mn^{IV}(O)$ in order to study their fundamental role in biomimetic oxidation reactions and synthetic catalytic cycles of practical significance.[5,6] High-valent manganese−oxo intermediates have also been implicated in the oxygen-evolving center of photosystem II.[7]

A number of studies involving high-valent manganese−oxo porphyrins have focused on their oxygen-atom-transfer reactivity with alkenes, halides, sulfides, PR_3, and NR_3 substrates as well as their C−H activation and hydride-transfer chemistry, and this work has included theoretical calculations.[8−13] In this regard, the higher-valent Mn^{V}−oxo porphyrins are more challenging to study than the Mn^{IV}−oxo complexes because of their inherent instability. In contrast, the Mn^{V}−oxo complexes of the ring-contracted porphyrinoids known as corrolazine and corrole show much better stability.[14,15] In particular, the $Mn^{V}(O)$ corrolazine (TBP_8Cz)-$Mn^{V}(O)$ (**1**) (TBP_8Cz = octa-*tert*-butylphenylcorrolazinato) is remarkably stable at room temperature and can be isolated as a solid following conventional benchtop chromatography.[16,17]

Received: September 16, 2010
Published: January 10, 2011

Scheme 1

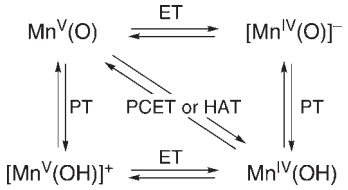

The mechanism of the C−H bond-cleaving step in oxidations mediated by high-valent metal−oxo complexes can involve hydrogen-atom transfer (HAT), hydride transfer, or electron transfer (ET). Determining the factors that control these different reaction pathways and favor one pathway over another is critical to our understanding of biomimetic oxidations.[18] However, these factors remain poorly understood, especially for transient species such as manganese(V)−oxo porphyrins. Previously, the mechanism of HAT with the manganese(V)−oxo corrolazine complex **1** was examined in some detail for both O−H substrates (2,6-*t*-Bu-4-X-phenols) and C−H substrates (1,4-cyclohexadiene and 9,10-dihydroanthracene).[19] Electrochemical measurements indicated that **1** is a relatively weak oxidant (0.02 V vs SCE), suggesting that the thermodynamic driving force for the oxidation of O−H and C−H substrates, which proceeds through a HAT mechanism, is significantly enhanced by the basicity of the incipient $[Mn^{IV}(O)]^-$ species. The thermodynamics of the HAT process can be analyzed in terms of the ET and proton-transfer (PT) steps shown in Scheme 1. It was suggested that the proton affinity of the Mn−oxo unit, represented by the thermodynamic favorability of the PT step on the right side of the square, allows **1** to overcome a low oxidation potential, represented by the ET step at the top. In more recent work, these findings were supported by the observation of unprecedented rate enhancements for C−H activation by the addition of anionic axial ligands to **1**.[19c] Theoretical calculations indicated that the addition of anionic donors should decrease the oxidation potential of **1** but also increase the proton affinity to an even larger extent, thereby providing the dramatic rate enhancements found experimentally for HAT. It should also be noted that the initial intermediate following HAT to **1** is postulated to be the $Mn^{IV}(OH)$ complex, but this species has not been observed during HAT to **1**. The data indicate that a second fast HAT step occurs, giving the $Mn^{III}(Cz)$ product. These results imply that the $Mn^{IV}(OH)$ complex may be a highly efficient oxidant in its own right.

In this study, we examined the electron-transfer properties of the $Mn^{V}(O)$ complex **1** with a series of one-electron reductants (ferrocene derivatives) and its hydride-transfer properties with a series of NADH analogues [10-methyl-9,10-dihydroacridine ($AcrH_2$), its 9-ethyl-substituted derivative (AcrHEt), 1-benzyl-1,4-dihydronicotinamide (BNAH), and their deuterated derivatives]. This work provides the first fundamental information on the ET properties of an isolated $Mn^{V}(O)$ complex as well as the first direct measurements of hydride-transfer kinetics with a $Mn^{V}(O)$ complex.

The driving-force dependence of the electron-transfer rate constant was analyzed in light of the Marcus theory of electron transfer,[20] leading to the evaluation of the reorganization energy of electron transfer for **1**. The effects of proton donors (e.g., CH_3CO_2H, CF_3CH_2OH, and CH_3OH) on an endergonic ET reaction with one of the ferrocene derivatives were also examined to clarify the proton-coupled electron transfer (PCET) mechanism. Earlier studies examined the ET properties of the oxomanganese(IV) porphyrin complex $(TMP)Mn^{IV}(O)$ (TMP = 5,10,15,20-tetrakis(2,4,6-trimethylphenyl)porphinato dianion),[13] which are compared with those of **1** in this study. The hydride-transfer reactivity is also compared with those of the dioxomanganese(V) porphyrin complex $[(TPFPP)Mn^{V}(O)_2]^-$ (TPFPP = *meso*-tetrakis(pentafluorophenyl)porphinato dianion)[9b] and an organic *p*-benzoquinone derivative.[21] The accessibility of the stable $Mn^{V}(O)$ corrolazine **1** provides a rare opportunity to examine the electron-transfer and hydride-transfer reactivities of a $Mn^{V}(O)$ complex, and comparison with the $Mn^{IV}(O)$ and $Mn^{V}(O)_2$ porphyrin complexes provides valuable insights into the mechanism of high-valent metal−oxo-mediated oxidations. The compounds investigated in this study are presented in Chart 1.

EXPERIMENTAL SECTION

Materials. The starting material $(TBP_8Cz)Mn^{III}$ was synthesized according to published procedures.[16] The commercially available reagents octamethylferrocene, 1,1′-dimethylferrocene, decamethylferrocene (Fc*), 10-methylacridone, acridine, 1-benzyl-1,4-dihydronicotinamide (BNAH), $(p\text{-}BrC_6H_4)_3N^{+\bullet}SbCl_6^-$, methyl iodide (MeI), $NaBH_4$, $LiAlD_4$ (CIL, Inc.), CH_3CO_2H, CF_3CH_2OH, and CH_3OH were of the best available purity and used without further purification unless otherwise noted. Toluene and dichloromethane were purified via a Pure-solv solvent purification system from Innovative Technologies, Inc. Benzonitrile (PhCN) and diethyl ether were dried according to literature procedures and distilled under Ar prior to use.[22] 9,10-Dihydro-10-methylacridine ($AcrH_2$) was prepared from 10-methylacridinium iodide ($AcrH^+I^-$) by reduction with $NaBH_4$ in methanol and purified by recrystallization from ethanol. $AcrH^+I^-$ was prepared by the reaction of acridine with methyl iodide in acetone and purified by recrystallization from methanol. The dideuterated compound [9,9′-$^2H_2$]-10-methylacridine ($AcrD_2$) was prepared from 10-methylacridone by reduction with $LiAlD_4$ in ether.[23] 9-Ethyl-9,10-dihydro-10-methylacridine was prepared by the reduction of $AcrH^+I^-$ with Grignard reagent (EtMgBr).[23] The dideuterated compound 1-benzyl-1,4-dihydro-[4,4′-$^2H_2$]nicotinamide (BNAH-4,4′-d_2) was prepared from the monodeuterated compound (BNAH-4-d_1) by three cycles of oxidation with *p*-chloranil in dimethylformamide and reduction with dithionite in deuterium oxide.[24]

$(TBP_8Cz)Mn^{V}(O)$ (1). The original synthesis of this complex was reported previously,[17] and the preparation is repeated here for convenience. Excess PhIO (0.763 g, 3.471 mmol) was added to a solution of $(TBP_8Cz)Mn^{III}$ (0.50 g, 0.347 mmol) in CH_2Cl_2 (25 mL), and the reaction mixture was stirred at room temperature for 30 min. PhIO is only sparingly soluble in CH_2Cl_2, and thus, an excess was added to ensure the complete oxidation of $(TBP_8Cz)Mn^{III}$. The solution changed from dark-green-brown to deep-green. The reaction was monitored by UV−vis spectroscopy to confirm the complete conversion of $(TBP_8Cz)Mn^{III}$ to **1**. The solvent was then removed on a rotary evaporator, and the residue was purified by column chromatography (CH_2Cl_2, silica gel) to give **1** as a dark-green solid. Any unreacted PhIO, which is mostly insoluble, was easily removed by the column purification of **1**. Complex **1** is diamagnetic, and its ^1H NMR spectrum and other analytical data have been reported previously.[16b]

Spectral and Kinetic Measurements. Hydride-transfer reactions involving the NADH analogues and **1** were carried out by the following representative procedure for $AcrH_2$. The reaction of $AcrH_2$ and **1** (1.0×10^{-6} M) was examined by monitoring spectral changes in the presence of an appropriate amount of $AcrH_2$ (6.5×10^{-5} to

Chart 1

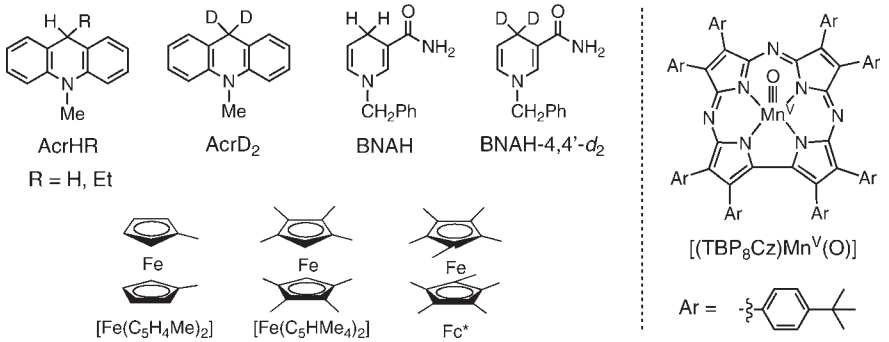

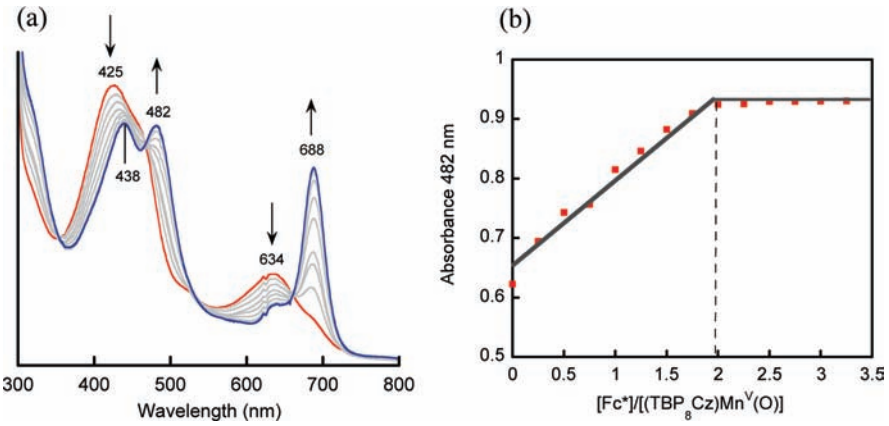

Figure 1. (a) UV−vis spectral changes in electron transfer from Fc* to **1** (1.9×10^{-5} M) in PhCN at 298 K. (b) Spectral titration to determine the stoichiometry of the electron-transfer reaction.

2.6×10^{-4} M) at 298 K using a Hewlett-Packard 8453 photodiode-array spectrophotometer and a quartz cuvette (path length = 10 mm). Typically, a deaerated PhCN solution of $AcrH_2$ was added with a microsyringe to a deaerated PhCN solution containing **1**. Kinetic measurements were performed on a UNISOKU RSP-601 stopped-flow spectrometer equipped with a MOS-type highly sensitive photodiode array or a Hewlett-Packard 8453 photodiode-array spectrophotometer at 298 K. Rates of electron transfer from Fc*, octamethylferrocene, and 1,1′-dimethylferrocene to **1** were monitored by either the increase in the absorption band due to $[(TBP_8Cz)Mn^{III}(OH)]^-$ ($[\mathbf{2\text{-}OH}]^-$) (λ_{max} = 688 nm, $\varepsilon_{max} = 3.5 \times 10^4$ M^{-1} cm^{-1}) or by the decrease in absorbance due to **1** (λ_{max} = 634 nm, $\varepsilon_{max} = 2.0 \times 10^4$ M^{-1} cm^{-1}). The concentration of ferrocene derivatives were maintained in more than 10-fold excess with respect to **1** for all kinetic measurements in order to ensure pseudo-first-order conditions.

Electrochemistry. High-purity N_2 was used to deoxygenate the PhCN solution before the electrochemical experiments were performed. Tetra-*n*-butylammonium hexafluorophosphate ($TBAPF_6$) was purchased from Sigma-Aldrich, recrystallized from ethyl alcohol, and dried under vacuum prior to use. Cyclic voltammetry was conducted with an EG&G model 263A potentiostat. A three-electrode system consisting of a glassy carbon working electrode, a platinum counter electrode, and a Ag/$AgNO_3$ 0.01 M reference electrode was used. All of the redox potentials (vs Ag/$AgNO_3$) were converted to values vs the saturated calomel electrode (SCE) by adding 0.29 V. Redox potentials were determined using the relation $E_{1/2} = (E_{pa} + E_{pc})/2$.

Generation of $(TBP_8Cz)Mn^{IV}(OH)$. To a solution of $(TBP_8Cz)Mn^{III}$ (1 mM) in toluene was added excess $Me_4N^+OH^- \cdot 5H_2O$ (solid, partially soluble). The solution was stirred for 30 min and then filtered through Celite and transferred to a Wilmad quartz EPR tube (3 mm i.d.). The sample was deaerated and remained under an argon atmosphere as 1 equiv of $(p\text{-}BrC_6H_4)_3N^{+\bullet}SbCl_6^-$ (1 mM) was added. The contents of the tube were mixed, and a color change from green-brown to brown was observed. After 1 h, the sample was frozen and stored at 77 K. Electron paramagnetic resonance (EPR) spectroscopy experiments were performed on a Bruker EMX spectrometer controlled with a Bruker ER 041 X G microwave bridge and equipped with a continuous-flow liquid helium cryostat (ESR900) coupled to an Oxford Instruments TC503 temperature controller. The spectra were obtained at 15 K under nonsaturating microwave power conditions (ν = 9.475 GHz, microwave power = 15.98 mW, modulation amplitude = 10 G, modulation frequency = 100 kHz). Spectral simulation was performed using Bruker WINEPR SimFonia software (version 1.26). UV−vis spectral titrations showing the interconversion of the Mn^{III} and Mn^{IV} complexes were performed by adding 0.25−2 equiv of $(p\text{-}BrC_6H_4)_3N^{+\bullet}SbCl_6^-$ (from a 1.8 mM stock solution in CH_2Cl_2) to **2** (18 μM) in CH_2Cl_2 (3 mL). A 10 min equilibration time was allotted between aliquots, until there were no further changes in absorbance. Isosbestic conversion was observed from 0.25 to 1 equiv, and no further changes in absorption were seen beyond 1 equiv. Addition of 0.25−1 equiv of cobaltocene (from a 1.8 mM stock solution in CH_2Cl_2) resulted in the regeneration of **2**.

RESULTS AND DISCUSSION

Electron Transfer from Ferrocene Derivatives to $(TBP_8Cz)Mn^{V}(O)$. When a one-electron reductant such as decamethylferrocene (Fc*) was employed, electron transfer from Fc* to $(TBP_8Cz)Mn^{V}(O)$ (**1**) occurred, producing the

dx.doi.org/10.1021/ja108395g |J. Am. Chem. Soc. 2011, 133, 1859–1869

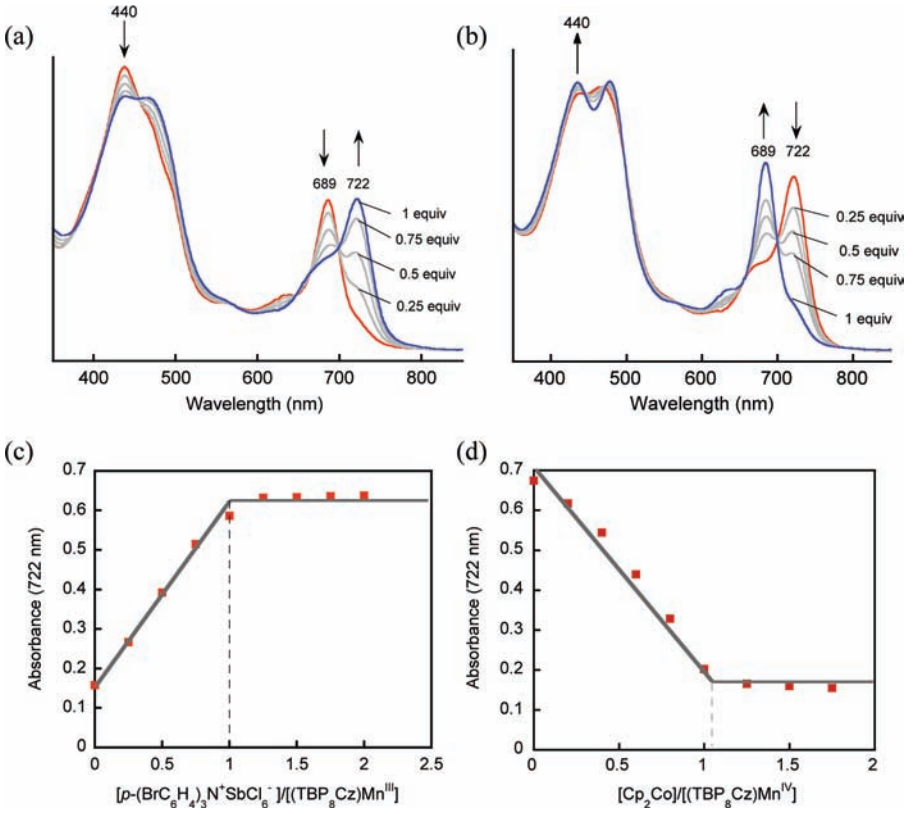

Figure 2. (a, b) UV−vis spectral changes observed in the electron-transfer reactions of (a) $(TBP_8Cz)Mn^{III}$ with $(p\text{-}BrC_6H_4)_3N^{\bullet+}SbCl_6^-$ and (b) $[(TBP_8Cz)Mn^{IV}]^+$ with Cp_2Co in CH_2Cl_2. (c, d) Spectral titrations to determine the stoichiometry of the electron-transfer reactions in (a) and (b), respectively.

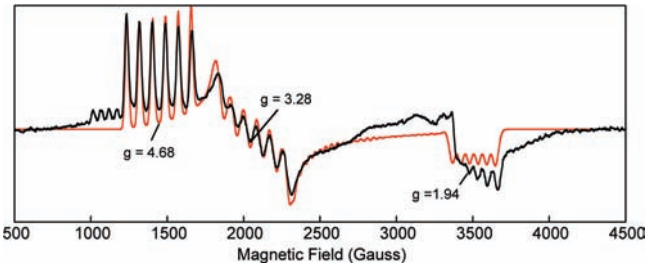

Figure 3. X-band EPR spectrum at 15 K of **3-OH** produced by the addition of $(p\text{-}BrC_6H_4)_3N^{\bullet+}SbCl_6^-$ to a solution of $[\mathbf{2\text{-}OH}]^-$ in toluene. The experimental spectrum is shown in black and the spectral simulation in red. Parameters for simulation: $S' = {}^1/_2$; $\mathbf{g}' = [4.68, 3.28, 1.94]$; $\mathbf{A}' = [84, 86, 56]$ G; Lorentzian line widths $W = 23$, 55, and 42 G.

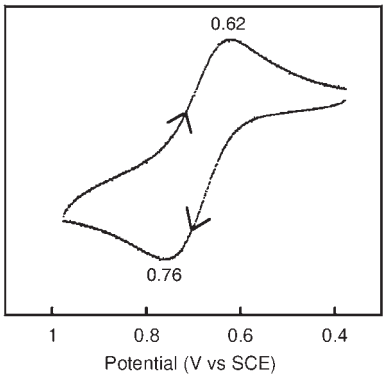

Figure 4. Cyclic voltammogram of $[\mathbf{2\text{-}OH}]^-$ (2.0×10^{-3} M) after the addition of Et_4NOH (2.0×10^{-3} M) to a solution of **2** (2.0×10^{-3} M) in PhCN containing 0.1 M $TBAPF_6$ with a glassy carbon working electrode at 298 K. The sweep rate was 25 mV s^{-1}.

corresponding ferrocenium ion (Fc^{*+}) and $[(TBP_8Cz)Mn^{III}(OH)]^-$ ($[\mathbf{2\text{-}OH}]^-$) as a two-electron reduced product (eq 1):

$$(TBP_8Cz)Mn^{V}(O) + 2Fc^{*} + H_2O \xrightarrow{PhCN} [(TBP_8Cz)Mn^{III}(OH)]^- + 2Fc^{*+} + OH^- \quad (1)$$

As shown in Figure 1a, the absorption band at 634 nm associated with **1** decreased smoothly, accompanied by an increase in the absorption bands at 482 and 688 nm. The latter bands are assigned to $[\mathbf{2\text{-}OH}]^-$, in agreement with the spectrum obtained from addition of Et_4NOH to $(TBP_8Cz)Mn^{III}$ in PhCN (see Figure S1 in the Supporting Information). A Job's plot analysis of the binding of OH^- to $(TBP_8Cz)Mn^{III}$ revealed a 1:1 stoichiometry, confirming the formulation of $[\mathbf{2\text{-}OH}]^-$ (Figure S1). The stoichiometry of the electron-transfer reaction (eq 1) was confirmed by performing a spectral titration at 482 nm (Figure 1b). Because the spectral change in going from **1** to $[\mathbf{2\text{-}OH}]^-$ in Figure 1a exhibited clean isosbestic points, the two-electron reduction of **1** occurred without any significant buildup of the one-electron-reduced species $[(TBP_8Cz)Mn^{IV}(O)]^-$.

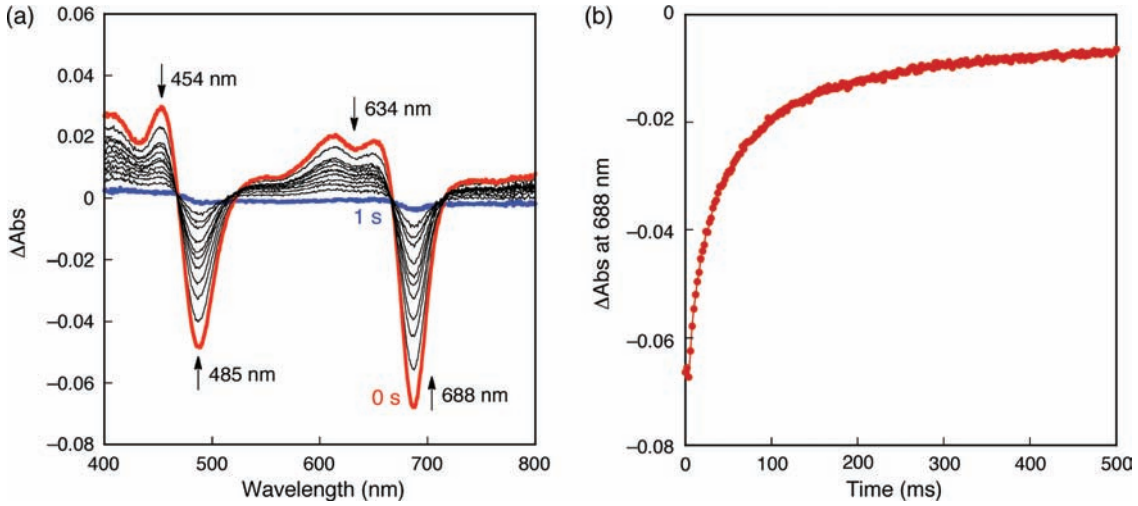

Figure 5. (a) UV−vis spectral changes observed in electron transfer from $[Fe(C_5HMe_4)_2]$ (2.4×10^{-4} M) to **1** (1.0×10^{-6} M) in PhCN at 298 K. It should be noted that the difference spectra were obtained with respect to the spectrum after the reaction. (b) Time profile of the absorbance at 688 nm due to $[\mathbf{2\text{-}OH}]^-$ along with a nonlinear fit to a single-exponential kinetic equation.

Table 1. Oxidation Potentials (E_{ox}) of Ferrocene Derivatives and Rate Constants (k_{et}) and Reorganization Energies (λ) for Electron Transfer from Ferrocene Derivatives to 1 in PhCN and (TMP)Mn^{IV}(O) in MeCN at 298 K

		$(TBP_8Cz)Mn^V(O)$		$(TMP)Mn^{IV}(O)$[c]	
ferrocene derivative	E_{ox} (V vs SCE)[a]	k_{et} (M^{-1} s^{-1})	λ (eV)	k_{et} (M^{-1} s^{-1})	λ (eV)
Fc*	−0.08	$(8.3 \pm 0.5) \times 10^5$	1.46 ± 0.04	n.d.	n.d.
$[Fe(C_5HMe_4)_2]$	−0.04	$(7.5 \pm 0.4) \times 10^4$	1.56 ± 0.07	n.d.	n.d.
$[Fe(C_5H_4Me)_2]$	0.26	$(1.1 \pm 0.2) \times 10^2$ [b]	1.58 ± 0.07	$(9.2 \pm 0.9) \times 10^5$	1.80 ± 0.10
$[Fe(C_5H_5)_2]$	0.37	n.d.	n.d.	$(3.2 \pm 0.2) \times 10^5$	1.72 ± 0.09
$[Fe(C_5H_5)(C_5BrH_4)]$	0.54	n.d.	n.d.	$(4.3 \pm 0.3) \times 10^4$	1.62 ± 0.07

[a] Data taken from refs 13 and 30. [b] The k_{et} value was determined as the saturation value in the plot of k_{et} vs $[CH_3CO_2H]$ in Figure 7. [c] Data taken from ref 13.

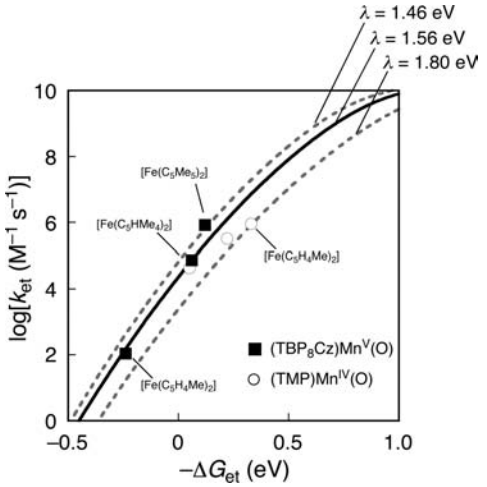

Figure 6. Dependence of $\log(k_{et}/M^{-1}\ s^{-1})$ on $-\Delta G_{et}$ for electron transfer from ferrocene derivatives to **1** in PhCN (■) and to (TMP)Mn^{IV}(O) in MeCN (○) at 298 K.

These data are consistent with the notion that $[(TBP_8Cz)Mn^{IV}(O)]^-$ is strongly basic and likely abstracts a proton from residual water to afford $(TBP_8Cz)Mn^{IV}(OH)$. This complex is then readily reduced by Fc* to yield $[\mathbf{2\text{-}OH}]^-$ as the final product. The strong influence of proton donors on the ET reaction was confirmed (see below).

The absence of any spectral evidence for the one-electron-reduced intermediates $[(TBP_8Cz)Mn^{IV}(O)]^-$ and $(TBP_8Cz)Mn^{IV}(OH)$ upon reduction of **1** by Fc* motivated us to find alternative methods for preparing such species. We considered the possibility of generating a Mn^{IV} complex in the absence of reductants. We speculated that perhaps addition of an appropriate oxidant to the Mn^{III} complex (**2**) would provide access to a Mn^{IV} species. The reaction of **2** with the strong one-electron oxidant $(p\text{-}BrC_6H_4)_3N^{\bullet+}SbCl_6^-$ resulted in the formation of a new species characterized by a sharp Q band at 722 nm (Figure 2a), as shown in the forward step of eq 2:

$$(TBP_8Cz)Mn^{III} \underset{Cp_2Co/CH_2Cl_2}{\overset{(p\text{-}BrC_6H_4)_3N^{+\bullet}SbCl_6^-}{\rightleftharpoons}} [(TBP_8Cz)Mn^{IV}]^+ \quad (2)$$

This Q-band was well-separated from bands due to either the Mn^{III} complex **2** or the Mn^V(O) complex **1** and did not match those of any other Mn corrolazines,[17,19] consistent with the conclusion that it arose from a new (Cz)Mn oxidation state. The 722 nm species immediately reacted with the one-electron reductant Cp_2Co^{II} to regenerate **2** (eq 2 and Figure 2b). Both the oxidation and reduction reactions occurred with good isosbestic behavior, and the 1:1 stoichiometry of these reactions

dx.doi.org/10.1021/ja108395g | J. Am. Chem. Soc. 2011, 133, 1859–1869

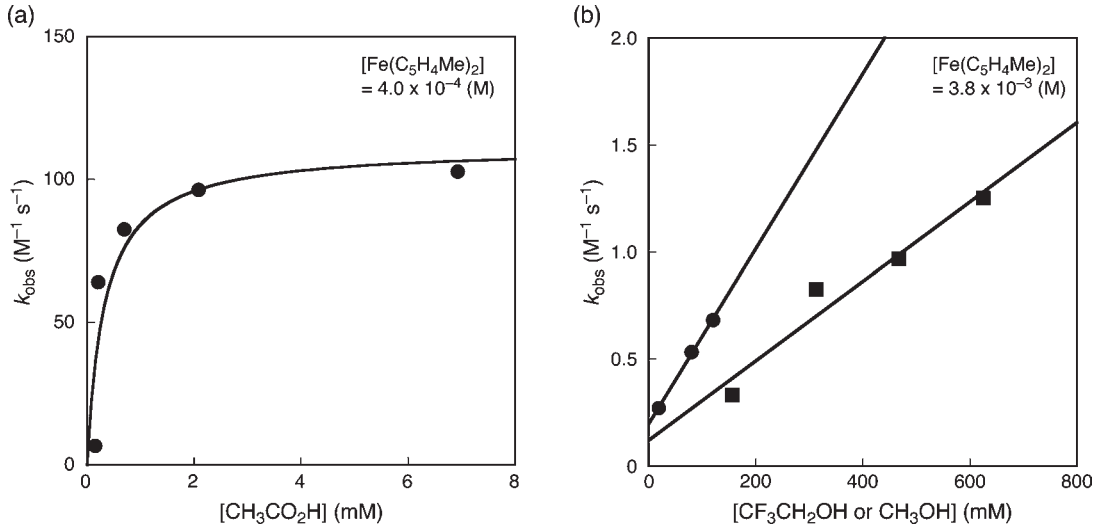

Figure 7. Plots of the rate constants (k_{obs}) of electron transfer from $[Fe(C_5H_4Me)_2]$ to **1** (1.0×10^{-6} M) as functions of (a) $[CH_3CO_2H]$ and (b) $[CF_3CH_2OH]$ (●) or $[CH_3OH]$ (■) in PhCN at 298 K.

was confirmed by spectral titrations (Figure 2c,d). These data indicate that a one-electron-oxidized species, formally the manganese(IV) complex $[(TBP_8Cz)Mn^{IV}]^+$ (**3**), is generated upon treatment of **2** with $(p\text{-}BrC_6H_4)_3N^{\bullet+}SbCl_6^-$. Attempts to isolate the Mn(IV) complex as a solid were not successful, leading instead to recovery of Mn(III). Thus, it appears that Mn(IV) corrolazine is not stable at high concentrations or in the solid state.

Confirmation that **3** contains a manganese ion in the +4 oxidation state was obtained by low-temperature EPR spectroscopy, as shown in Figure 3. The oxidation of **2** for EPR measurements was done in the presence of excess Et_4NOH. Under these conditions, **2** is quantitatively bound by OH^- to give $[\mathbf{2\text{-}OH}]^-$, and one-electron oxidation was expected to generate $(TBP_8Cz)Mn^{IV}(OH)$ (**3-OH**), although direct evidence for the presence of the axial OH^- in the oxidized product was not obtained. The well-resolved rhombic spectrum in Figure 3 provides conclusive evidence for the formation of a high-spin Mn^{IV} (d^3, $S = {}^3/_2$) complex.[25] Similar EPR spectra were also obtained when **2** was oxidized in the absence of added OH^-, but the Mn hyperfine coupling was less apparent. These results suggest that intermolecular interactions may become more significant in the absence of a strong axial donor such as OH^-, perhaps through π-stacking effects. Simulation of the spectrum in Figure 3 assuming a fictitious spin of $S' = {}^1/_2$ gave effective g' values of $g'_{max} = 4.68$, $g'_{mid} = 3.28$, and $g'_{min} = 1.94$ and ^{55}Mn hyperfine coupling constants of $A_{g_{max}}{}' = 84$, $A_{g_{mid}}{}' = 86$, and $A_{g_{min}}{}' = 56$ G. These parameters can be compared to those of the Mn^{IV} corrole $[(tpfc)Mn^{IV}]^+$ [tpfc = 5,10,15-tris-(pentafluorophenyl)corrole], which were reported to be $g'_{max} = 4.57$, $g'_{mid} = 3.60$, and $g'_{min} = 1.995$ (the A values were not given),[25a] and those of the Mn^{IV} porphyrin $(TPP)Mn^{IV}(OCH_3)_2$ (TPP = tetraphenylporphyrin), which were reported to be $g'_{max} = 5.43$, $g'_{mid} = 2.4$, $g'_{min} = 1.6$, and $A_{g_{max}}{}' = 72$ G ($A_{g_{mid}}{}'$ and $A_{g_{min}}{}'$ were not resolved).[25b]

A perturbation theory approach, as described by Banci et al.,[26] was applied to the spectrum of **3-OH** in order to analyze the effective g' values in terms of the zero-field splitting (ZFS) parameters D and E for an $S = {}^3/_2$ ion. Although this approach was developed by Banci et al. for EPR spectra arising from tetrahedral Co^{II}, it is appropriate here because of the equivalent ground states $[(t_2)^3]$ for tetrahedral Co^{II} and square-pyramidal (distorted octahedral) Mn^{IV} ions. With a relatively large, positive D value ($D \gg 0.5$ cm^{-1}) and an intrinsic, isotropic g value of 2.00 for Mn^{IV}, use of the perturbation equations with $E/D = 0.115$ led to the calculated g' values $g'_y = 4.64$, $g'_x = 3.28$, and $g'_z = 1.92$ for the lower Kramers doublet ($M_S = \pm{}^1/_2$). These g values are in good agreement with those obtained in Figure 3. In comparison, a five-coordinate Mn^{IV} complex with trigonal-bipyramidal symmetry prepared by Borovik and co-workers[27] gave an EPR spectrum that was simulated with $E/D = 0.26$. The larger rhombicity in this case may not be surprising in view of the lower symmetry of this complex. There is also an additional six-line feature at the low-field edge of the spectrum in Figure 3 that can be assigned to the upper Kramers doublet ($M_S = \pm{}^3/_2$). A similar feature was derived from the simulation of the spectrum by Borovik and co-workers. More detailed studies, such as high-field and high-frequency EPR spectroscopy measurements,[28] are needed to definitively obtain the ZFS parameters, particularly the magnitude of D, but it is clear that **3-OH** is an $S = {}^3/_2$ Mn^{IV} complex.

The one-electron oxidation potential of $[(TBP_8Cz)Mn^{III}(OH)]^-$ in PhCN was determined to be 0.69 V (vs SCE), as shown by the cyclic voltammogram in Figure 4, which reveals a reversible redox wave for the Mn^{IV}/Mn^{III} couple. The value of $E_{1/2}$ was found to be independent of the scan rate (ν), while the current was shown to be proportional to $\nu^{1/2}$. Thus, electron transfer from the Mn^{III} complex **2** to the strong

Scheme 2

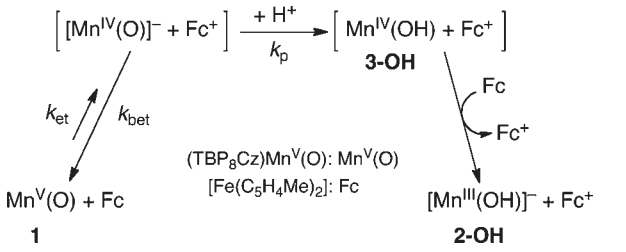

dx.doi.org/10.1021/ja108395g |J. Am. Chem. Soc. 2011, 133, 1859–1869

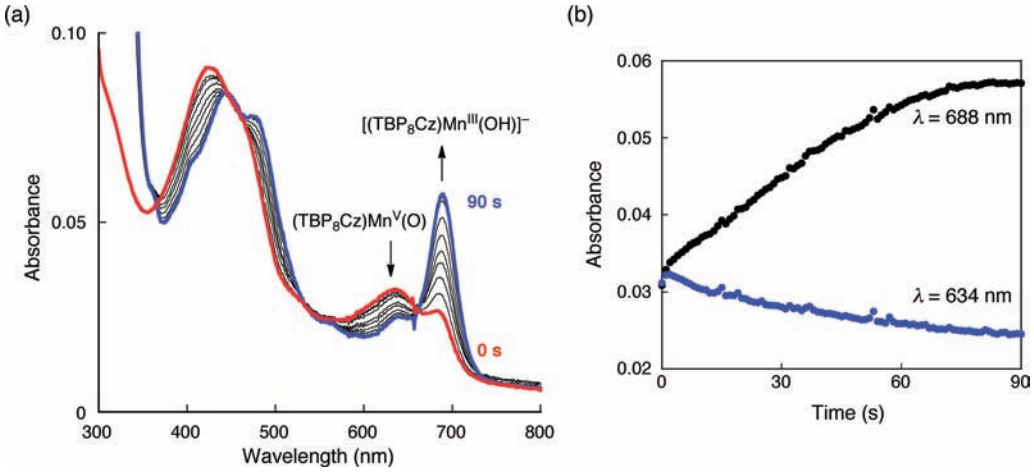

Figure 8. (a) Spectral changes observed in the reaction of **1** (1.0×10^{-6} M) and $AcrH_2$ (2.5×10^{-4} M) in deaerated PhCN at 298 K. (b) Time profiles of absorption changes at λ = 688 and 634 nm for the formation of $[\mathbf{2\text{-}OH}]^-$ and decay of **1**, respectively.

one-electron oxidant $(p\text{-}BrC_6H_4)_3N^{\bullet+}SbCl_6^-$ (1.05 V vs SCE)[29] as shown in eq 2 is thermodynamically feasible. On the basis of the one-electron reduction potential of **3-OH**, which is equivalent to the one-electron oxidation potential of $[\mathbf{2\text{-}OH}]^-$ (0.69 V vs SCE), the second electron transfer from the ferrocene derivatives to **3-OH** must be much faster than the first electron transfer from Fc to **1**.

Further insights into the mechanism of electron transfer between the ferrocene derivatives and **1** were obtained from kinetic measurements. The rate of formation of $[\mathbf{2\text{-}OH}]^-$ via ET from $[Fe(C_5HMe_4)_2]$ to **1** was determined from the increase in absorbance at 688 nm using a stopped-flow technique, which coincided with the decay rate of **1** determined from a decrease in absorbance at 634 nm (Figure 5). The formation rate of $[\mathbf{2\text{-}OH}]^-$ obeyed first-order kinetics, and the pseudo-first-order rate constant (k_{obs}) increased linearly with increasing $[Fe(C_5HMe_4)_2]$ concentration (Figure S2 in the Supporting Information).

The observed single-exponential kinetics indicates that the first electron transfer from $[Fe(C_5HMe_4)_2]$ to **1** is the rate-determining step and that this is followed by facile protonation and the second electron transfer from $[Fe(C_5HMe_4)_2]$ to $(TBP_8Cz)Mn^{IV}(OH)$, as expected on the basis of the thermodynamics mentioned above. The second-order rate constant (k_{et}) of electron transfer from $[Fe(C_5HMe_4)_2]$ to **1** was determined to be $(7.5 \pm 0.4) \times 10^4$ M^{-1} s^{-1}. The kinetics of electron transfer were similarly examined for the ferrocene derivatives Fc* and $[Fe(C_5H_4Me)_2]$ to determine the second-order rate constants of electron transfer (k_{et}) in reaction with **1** (Table 1).

The driving-force dependence of the rate constants of electron transfer from ferrocene derivatives to **1** in PhCN at 298 K is shown in Figure 6, where the log k_{et} values are plotted against the $-\Delta G_{et}$ values. The driving force of electron transfer from ferrocene derivatives to **1** was determined using eq 3:

$$-\Delta G_{et} = e(E_{red} - E_{ox}) \quad (3)$$

where E_{ox} is the one-electron oxidation potential of the ferrocene derivative and E_{red} is the one-electron reduction potential of **1**.[13,30] The E_{red} value of **1** was already determined to be 0.02 V vs SCE in PhCN. Each curve was well-fitted by the solid line obtained using the Marcus theory of adiabatic outer-sphere

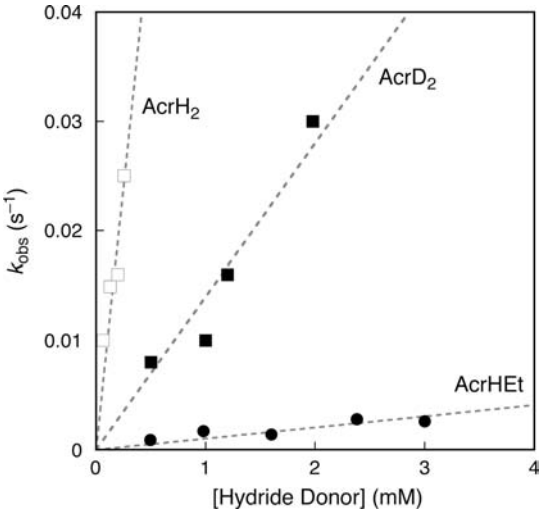

Figure 9. Plots of the observed pseudo-first-order rate constant (k_{obs}) of hydride transfer from NADH analogues to **1** (1.0×10^{-6} M) in the presence of (□) $AcrH_2$ (6.5×10^{-5} to 2.6×10^{-4} M), (■) $AcrD_2$ (5.0×10^{-4} to 2.0×10^{-3} M), and (●) AcrEt (5.0×10^{-4} to 3.0×10^{-3} M) in deaerated PhCN at 298 K.

electron transfer (eq 4):

$$k_{et} = Z \exp\left[-\frac{\lambda}{4}\frac{(1+\Delta G_{et}/\lambda)^2}{k_B T}\right] \quad (4)$$

where λ is the reorganization energy of electron transfer, k_B is the Boltzmann constant, Z is the collision frequency (which was taken as 1×10^{11} M^{-1} s^{-1}), and T is the absolute temperature.[20] The λ value can be determined using eq 5, which is derived from eq 4:

$$\lambda = -\Delta G_{et} - 2RT \ln\left(\frac{k_{et}}{Z}\right) + \left\{\left[\Delta G_{et} + 2k_B T \ln\left(\frac{k_{et}}{Z}\right)\right]^2 - (\Delta G_{et})^2\right\}^{1/2} \quad (5)$$

Very similar λ values were obtained irrespective of the driving force as shown in Table 1, because ferrocene

dx.doi.org/10.1021/ja108395g |J. Am. Chem. Soc. 2011, 133, 1859–1869

Table 2. Oxidation Potentials (E_{ox}) of NADH Analogues and Rate Constants (k_H) for the Reactions of Hydride Transfer from NADH Analogues to Cl_4Q, $[(TBP_8Cz)Mn^V(O)]$ (1), and $[(TPFPP)Mn^V(O)_2]^-$ in Deaerated PhCN at 298 K

			k_H (M^{-1} s^{-1})		
entry	NADH analogue	E_{ox} (V vs SCE)[a]	Cl_4Q[a]	**1**[b]	$[(TPFPP)Mn^V(O)_2]^-$[c]
1	BNAH	0.57	1.0×10^3	2.0×10^4	1.3×10^3
2	BNAH-4,4′-d_2	0.57	1.9×10^2	1.4×10^3	1.4×10^2
3	$AcrH_2$	0.81	1.5×10	9.6×10	1.6×10
4	$AcrD_2$	0.81	1.7	1.4×10	1.3
5	AcrHMe	0.84	9.4×10^{-1}	–	3.4×10^{-1}
6	AcrHPh	0.88	6.6×10^{-1}	–	2.0×10^{-1}
7	AcrHEt	0.84	4.6×10^{-1}	1.3	1.2×10^{-1}

[a] Data taken from refs 21 and 37. [b] The experimental errors are within ±5%. [c] Data taken from ref 9b.

derivatives have similar reorganization energies of electron self-exchange.[31]

The k_{et} and λ values for the porphyrin complex (TMP)-$Mn^{IV}(O)$ are listed in Table 1 for comparison. The λ value for the electron-transfer reduction of **1** (av 1.53 ± 0.05 eV) is significantly smaller than the value found for $(TMP)Mn^{IV}(O)$ (av 1.71 ± 0.09 eV).[13] An even greater contrast can be seen when one compares the values for **1** with the recently obtained λ values for non-heme iron(IV)−oxo complexes, which range between 1.97 and 2.74 eV.[30] The relatively small reorganization energy for **1** may be a reflection of the particularly flat and rigid corrolazine macrocycle, which suggests that synthetic modifications to increase the driving force of ET in metal−oxo corrolazines may be a good strategy for yielding exceptionally powerful oxidation catalysts.

Effect of Protons on Electron Transfer. As shown in eq 1, the presumed source of H^+ for the facile protonation of the reduced $[(TBP_8Cz)Mn^{IV}(O)]^-$ is residual H_2O. To further investigate the importance of protons in the reduction of the $Mn^V(O)$ complex, the rate of reaction between $[Fe(C_5H_4Me)_2]$ and **1** was determined in the presence of a series of proton donors. $[Fe(C_5H_4Me)_2]$ was selected as an electron donor for these experiments because its reaction with **1** is relatively slow and easily monitored by conventional UV−vis spectroscopy (Figure S3 in the Supporting Information). In addition, the driving force for the reaction between **1** and $[Fe(C_5H_4Me)_2]$ is slightly uphill (ΔG_{et} = 0.21 eV), so we anticipated that the effect of adding H^+ may be significant and easily observed as an increase in the reaction rate.

The two-electron reduction of **1** by $[Fe(C_5H_4Me)_2]$ was monitored in the presence of various amounts of three potential proton donors: CH_3CO_2H, CF_3CH_2OH, and CH_3OH. These three donors were selected because they span a large range of pK_a values, allowing us to address the influence of proton donation in some detail.[32] Addition of 10 equiv of CH_3CO_2H resulted in a 30-fold increase in the second-order rate constant for the conversion of **1** to $[$**2-OH**$]^-$. Clean isosbestic behavior was maintained, as shown in Figure S4 in the Supporting Information, indicating that the reaction proceeds in the same manner as in the absence of CH_3CO_2H with no evidence for the buildup of an intermediate. Addition of CH_3CO_2H to **1** in the absence of a reductant caused no UV−vis spectral change, indicating that **1** is not protonated under these conditions. The k_{obs} values for the reaction between **1** and excess $[Fe(C_5H_4Me)_2]$ increased with increasing concentration of CH_3CO_2H and exhibited saturation behavior, reaching a constant value (k_{et} = 110 M^{-1} s^{-1}) as shown in Figure 7. This saturation behavior is consistent with the mechanism shown in Scheme 2. In this case, the uphill nature of the ET reaction (k_{et}) implies that the ion-pair complex $[Mn^{IV}(O)^- + Fc^+]$ undergoes back-ET (k_{bet}) in competition with protonation of $[Mn^{IV}(O)]^-$ (k_p) followed by rapid electron transfer from Fc to **3-OH** (Mn^{IV}) to yield **2-OH** and Fc^+. A kinetic model based on Scheme 2 leads to the dependence of k_{obs} on $[H^+]$ as shown in eq 6:

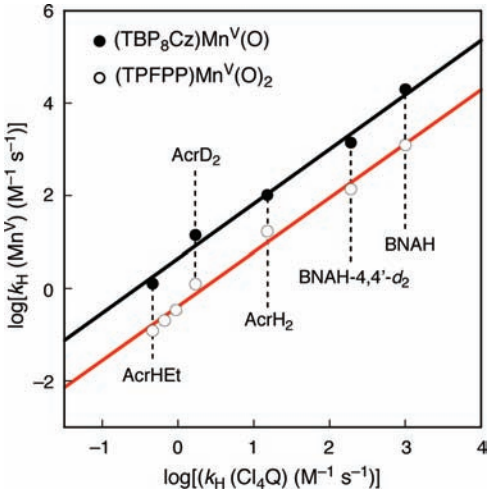

Figure 10. Plots of log k_H for hydride transfer from NADH analogues to **1** and $[(TPFPP)Mn^V(O)_2]^-$ vs log k_H for hydride transfer from the same series of NADH analogues to Cl_4Q in PhCN at 298 K.

$$k_{obs} = \frac{k_p k_{et}[H^+]}{k_{bet} + k_p[H^+]} \quad (6)$$

This indicates that the k_{obs} value should increase with increasing $[H^+]$ to reach a constant value equal to k_{et} (see the detailed derivation on p S5 in the Supporting Information). The k_{et} value of electron transfer from $[Fe(C_5H_4Me)_2]$ to **1** in Scheme 2 was obtained as the saturation value in Figure 7. The k_{et} value fits well with the driving-force dependence of k_{et} in Figure 6.

The addition of the weaker proton donors CF_3CH_2OH and CH_3OH also had an impact on the rate of reduction of **1** by $[Fe(C_5H_4Me)_2]$. In both cases, the reaction rates were linearly dependent on the concentration of the added proton donor at a fixed concentration of $[Fe(C_5H_4Me)_2]$ (Figure 7b). Second-order rate constants in the presence of these proton donors were

Scheme 3

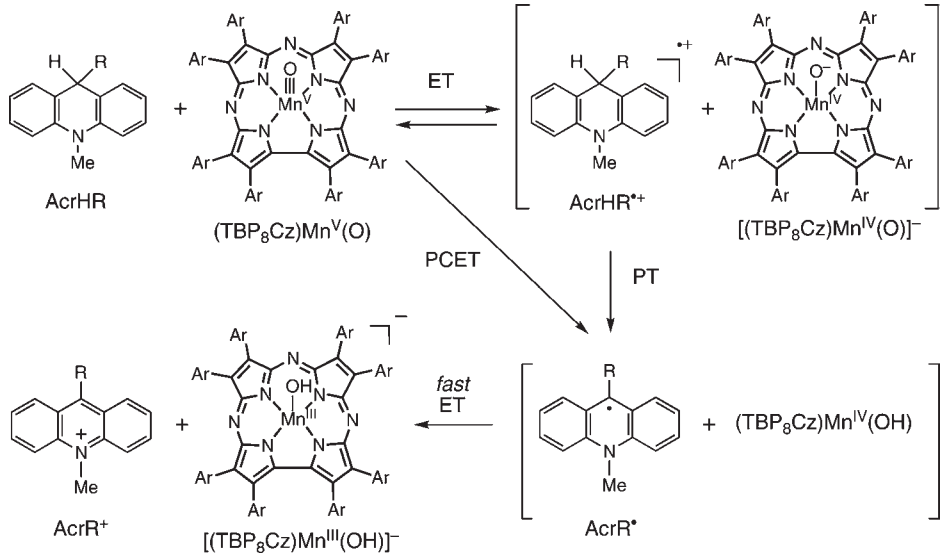

derived from plots of k_{obs} versus the concentration of $[Fe(C_5H_4Me)_2]$ (Figure S5b,c in the Supporting Information), which show a 7-fold increase in the rate constant using excess CF_3CH_2OH (10000 equiv) but only a 2-fold increase using excess CH_3OH (10000 equiv). There is a clear correlation between the pK_a of the proton source and the reaction rate, although a possible increase in the reactivity due to a change in the Mn(V/IV) reduction potential in the presence of a large amount of CH_3OH or CF_3CH_2OH has yet to be ruled out. These results support the proposed mechanism in Scheme 2, in which protonation of the $[Mn^{IV}(O)]^-$ species is critical to the initial rate-determining step for the reduction of **1** to $[\mathbf{2\text{-}OH}]^-$. These data also indicate that the reduction of **1** by ferrocene derivatives is formally a PCET process,[33−35] similar to the HAT reactions previously observed for **1**.[19]

Hydride Transfer from NADH Analogues to [(TBP$_8$Cz)Mn^V(O)]. Upon addition of an NADH analogue ($AcrH_2$) to the solution of **1**, UV−vis spectral changes were observed as shown in Figure 8. The spectrum after the reaction agreed well with the superposition of the $AcrH^+$ and $[\mathbf{2\text{-}OH}]^-$ spectra (Figure 8a). Thus, the stoichiometry of the reaction is given by eq 7:

$$(TBP_8Cz)Mn^V(O) + AcrH_2 \rightarrow [(TBP_8Cz)Mn^{III}(OH)]^- + AcrH^+ \quad (7)$$

The rate of formation of $[\mathbf{2\text{-}OH}]^-$ obeyed first-order kinetics, and the pseudo-first-order rate constant (k_{obs}) increased linearly with increasing $AcrH_2$ concentration (Figure 9). The second-order rate constant (k_H) for hydride transfer from $AcrH_2$ to **1** was determined to be $9.6 \times 10\ M^{-1}\ s^{-1}$ from the linear plot of k_{obs} versus $AcrH_2$ concentration. When $AcrH_2$ was replaced by the dideuterated compound $AcrD_2$, a kinetic deuterium isotope (KIE) value of 6.9 was observed. Hydride-transfer reactions using the NADH analogue BNAH and its deuterated analogue as well as an ethyl-substituted acridine (AcrHEt) were also investigated, and the k_H values are listed in Table 2.

Comparison of the Hydride-Transfer Reactivities of [(TBP$_8$Cz)Mn^V(O)] and *p*-Chloranil. The rate constants of hydride transfer from NADH analogues to **1** were compared with those of hydride transfer from the same series of NADH analogues to the organic oxidant *p*-chloranil (Cl_4Q) (Table 2).[21a] A good linear correlation between the log k_H values for **1** and the corresponding values for Cl_4Q was found, as shown by the black line in Figure 10, suggesting similar mechanisms of hydride transfer for **1** and Cl_4Q. For both **1** and Cl_4Q, there is a significant decrease in the ET rate upon substitution of an ethyl (Et) group at the C9 position of $AcrH_2$ (compare the log k_H values for AcrHEt vs $AcrH_2$). The Et group is electron-donating and would be expected to stabilize the carbocation intermediate arising from a concerted hydride-transfer mechanism, which in turn should lead to an *increase* in the reaction rate. It is also positioned in a boat axial conformation, which forces the hydrogen to be located in an equatorial position and minimizes the steric hindrance of the Et group on hydride transfer. Thus, the remarkable decrease in the H^- transfer rate for **1** induced by the addition of an Et group to C9 of $AcrH_2$ indicates that the rate-determining step for this reaction does not involve concerted H^- transfer.

There is a good linear correlation between the log k_H values for the *trans*-dioxomanganese(V) porphyrin $[(TPFPP)Mn^V(O)_2]^-$ and the corresponding values for Cl_4Q, as shown by the red line in Figure 10.[9b] The log k_H values for **1** are 10 times larger than the corresponding values for $[(TPFPP)Mn^V(O)_2]^-$. The lower reactivity for $[(TPFPP)Mn^V(O)_2]^-$ than for **1** may be a direct result of the additional oxo group in $[(TPFPP)Mn^V(O)_2]^-$. The hydride-transfer reactions for Cl_4Q and $[(TPFPP)Mn^V(O)_2]^-$ with NADH analogues have been shown to proceed through a rate-determining step involving PCET that is followed by fast ET from the resulting NAD radical analogue intermediates.[23,36−38] The parallel reactivity of **1** with both $[(TPFPP)Mn^V(O)_2]^-$ and Cl_4Q in Figure 10 suggests that the same mechanism is operative, i.e., that a slow PCET step is followed by fast ET from the resulting NAD$^\bullet$ analogues to

dx.doi.org/10.1021/ja108395g | J. Am. Chem. Soc. 2011, 133, 1859–1869

$(TBP_8Cz)Mn^{IV}(OH)$ to afford NAD^+ analogues and $[\mathbf{2\text{-}OH}]^-$, as shown in Scheme 3. The large kinetic isotope effects observed for both $AcrH_2$ and BNAH are consistent with a rate-determining step that involves C−H bond cleavage. Together with the previously described influence of the addition of the Et group on the acridine derivative, the kinetic data provide strong evidence for the PCET mechanism proposed in Scheme 3.

CONCLUSION

The electron-transfer properties of an isolated Mn^V−oxo complex have been measured for the first time. The ET from ferrocene derivatives to $(TBP_8Cz)Mn^V(O)$ (**1**) is followed by faster ET to $(TBP_8Cz)Mn^{IV}(OH)$, producing the two-electron-reduced species $[(TBP_8Cz)Mn^{III}(OH)]^-$ after facile protonation of $[(TBP_8Cz)Mn^{IV}(O)]^-$. Thus, $(TBP_8Cz)Mn^{IV}(OH)$ is much easier to reduce than $(TBP_8Cz)Mn^V(O)$, which suggests that the $Mn^{IV}(OH)$ complex is a more potent oxidant than the starting $Mn^V(O)$ complex. A Marcus analysis of the ET rates yielded reorganization energies (λ) for the electron-transfer reduction of **1** by three different ferrocene derivatives that are in close agreement with each other, with $\lambda_{av} = 1.53 \pm 0.05$ eV. This value is significantly smaller than the values found for the heme-related complex $(TMP)Mn^{IV}(O)$ (av 1.71 ± 0.09 eV) and a series of non-heme $Fe^{IV}(O)$ complexes (2.05−2.74 eV), suggesting that designing new metal−oxo corrolazines with greater oxidation potentials may lead to powerful oxidation catalysts. Despite the lack of direct spectroscopic evidence for $(TBP_8Cz)Mn^{IV}(OH)$ from the one-electron reduction of **1**, a manganese corrolazine in the +4 oxidation state was independently synthesized by the stoichiometric oxidation of $[\mathbf{2\text{-}OH}]^-$ with a one-electron oxidant. This oxidation yielded a new, distinct UV−vis absorbance at 722 nm and an EPR spectrum indicative of a Mn^{IV} (d^3, $S = {}^3/_2$) system. The presence of proton donors for the reduction of **1** with 1,1′-dimethylferrocene was found to directly influence the reaction rate. Increasing the pK_a of the proton donor resulted in higher rates of electron transfer ($CH_3OH < CF_3CH_2OH < CH_3CO_2H$), providing strong evidence that the reduction indeed proceeds by PCET and that protons are involved in the overall two-electron process. Complex **1** has been shown to be reactive toward a series of NADH analogues in formal hydride-transfer reactions. The logarithms of the observed second-order rate constants ($\log k_H$) of hydride transfer from the NADH analogues to **1** are linearly correlated with those of hydride transfer from the same series of NADH analogues to *p*-chloranil and $[(TPFPP)Mn^V(O)_2]^-$. For these latter oxidants, the hydride-transfer reactions have been shown previously to involve PCET followed by fast ET from $NAD^\bullet$ analogues, and it was concluded that hydride transfer to **1** involves the same mechanism. Although the Mn^V−oxo complex **1** is a mild one-electron oxidant, its ability to oxidize organic substrates appears to be enhanced by the significant basicity of the metal−oxo unit, which helps to drive the critical PCET process involved in C−H activation. In addition, a low reorganization energy may add to the oxidizing power of **1**.

ASSOCIATED CONTENT

Supporting Information. Figures S1−S5 and the derivation of eq 6. This material is available free of charge via the Internet at http://pubs.acs.org.

AUTHOR INFORMATION

Corresponding Author
fukuzumi@chem.eng.osaka-u.ac.jp; dpg@jhu.edu

ACKNOWLEDGMENT

This work was supported by the NSF (CHE0909587 to D. P.G.), by the NIH (GM62309 to D.P.G.), by a Grant-in-Aid (20108010) and a Global COE Program ("The Global Education and Research Center for Bio-Environmental Chemistry") from the Ministry of Education, Culture, Sports, Science, and Technology, Japan, and by KOSEF/MEST through the WCU Project (R31-2008-000-10010-0). K.A.P. is grateful for a Harry and Cleio Greer Fellowship. We thank Prof. Joshua Telser (Roosevelt University) for helpful comments.

REFERENCES

(1) Nam, W. *Acc. Chem. Res.* **2007,** *40,* 465 and review articles in the special issue.

(2) *Metal−Oxo and Metal−Peroxo Species in Catalytic Oxidations*; Meunier, B., Ed.; Springer-Verlag: Berlin, 2000.

(3) (a) van Eldik, R. *Coord. Chem. Rev.* **2007,** *251,* 1649–1662. (b) Nam, W. *Acc. Chem. Res.* **2007,** *40,* 522–531. (c) Shaik, S.; Hirao, H.; Kumar, D. *Acc. Chem. Res.* **2007,** *40,* 532–542. (d) Makris, T. M.; von Koenig, K.; Schlichting, I.; Sligar, S. G. *J. Inorg. Biochem.* **2006,** *100,* 507–518.

(4) (a) *Cytochrome P450: Structure, Mechanism, and Biochemistry,* 3rd ed.; Ortiz de Montellano, P. R., Ed.; Kluwer Academic/Plenum Publishers: New York, 2005. (b) Denisov, I. G.; Makris, T. M.; Sligar, S. G.; Schlichting, I. *Chem. Rev.* **2005,** *105,* 2253–2278. (c) Shaik, S.; Kumar, D.; de Visser, S. P.; Altun, A.; Thiel, W. *Chem. Rev.* **2005,** *105,* 2279–2328. (d) Meunier, B.; de Visser, S. P.; Shaik, S. *Chem. Rev.* **2004,** *104,* 3947–3980. (e) Groves, J. T. *Proc. Natl. Acad. Sci. U.S.A.* **2003,** *100,* 3569–3574. (f) Ortiz de Montellano, P. R.; De Voss, J. J. *Nat. Prod. Rep.* **2002,** *19,* 477–493.

(5) (a) Meunier, B. *Chem. Rev.* **1992,** *92,* 1411–1456. (b) Mansuy, D. *Coord. Chem. Rev.* **1993,** *125,* 129–141. (c) Groves, J. T. In *Cytochrome P450: Structure, Mechanism, and Biochemistry,* 3rd ed.; Ortiz de Montellano, P. R., Ed.; Kluwer Academic/Plenum Publishers: New York, 2005; pp 1−43. (d) Groves, J. T.; Lee, J.; Marla, S. S. *J. Am. Chem. Soc.* **1997,** *119,* 6269–6273. (e) Jin, N.; Groves, J. T. *J. Am. Chem. Soc.* **1999,** *121,* 2923–2924.

(6) (a) Jin, N.; Bourassa, J. L.; Tizio, S. C.; Groves, J. T. *Angew. Chem., Int. Ed.* **2000,** *39,* 3849–3851. (b) Nam, W.; Kim, I.; Lim, M. H.; Choi, H. J.; Lee, J. S.; Jang, H. G. *Chem.—Eur. J.* **2002,** *8,* 2067–2071. (c) Zhang, R.; Newcomb, M. *J. Am. Chem. Soc.* **2003,** *125,* 12418–12419. (d) Zhang, R.; Horner, J. H.; Newcomb, M. *J. Am. Chem. Soc.* **2005,** *127,* 6573–6582. (e) Shimazaki, Y.; Nagano, T.; Takesue, H.; Ye, B.-H.; Tani, F.; Naruta, Y. *Angew. Chem., Int. Ed.* **2004,** *43,* 98–100.

(7) (a) Betley, T. A.; Wu, Q.; Voorhis, T. V.; Nocera, D. G. *Inorg. Chem.* **2008,** *47,* 1849–1861. (b) Mullins, C.; Pecoraro, V. L. *Coord. Chem. Rev.* **2008,** *252,* 416–443. (c) Cady, C. W.; Crabtree, R. H.; Brudvig, G. W. *Coord. Chem. Rev.* **2008,** *252,* 444–455. (d) McEvoy, J. P.; Brudvig, G. W. *Chem. Rev.* **2006,** *106,* 4455–4483. (e) *Photosystem II: The Light-Driven Water:Plastoquinone Oxidoreductase*; Wydrzynski, T., Satoh, K., Eds.; Advances in Photosynthesis and Respiration, Vol. 22; Springer: Dordrecht, The Netherlands, 2005.

(8) (a) Groves, J. T.; Watanabe, Y.; McMurry, T. J. *J. Am. Chem. Soc.* **1983,** *105,* 4489–4490. (b) Jin, N.; Ibrahim, M.; Spiro, T. G.; Groves, J. T. *J. Am. Chem. Soc.* **2007,** *129,* 12416–12417. (c) Gross, Z. *Angew. Chem., Int. Ed.* **2008,** *47,* 2737–2739.

(9) (a) Song, W. J.; Seo, M. S.; George, S. D.; Ohta, T.; Song, R.; Kang, M.-J.; Tosha, T.; Kitagawa, T.; Solomon, E. I.; Nam, W. *J. Am. Chem. Soc.* **2007,** *129*, 1268–1277. (b) Lee, J. Y.; Lee, Y.-M.; Kotani, H.; Nam, W.; Fukuzumi, S. *Chem. Commun.* **2009,** 704–706.

(10) (a) Balcells, D.; Raynaud, C.; Crabtree, R. H.; Eisenstein, O. *Chem. Commun.* **2009,** 1772–1774. (b) Balcells, D.; Raynaud, C.; Crabtree, R. H.; Eisenstein, O. *Chem. Commun.* **2008,** 744–746. (c) De Angelis, F.; Jin, N.; Car, R.; Groves, J. T. *Inorg. Chem.* **2006,** *45*, 4268–4276. (d) de Visser, S. P.; Ogliaro, F.; Gross, Z.; Shaik, S. *Chem.—Eur. J.* **2001,** *7*, 4954–4960.

(11) (a) Lahaye, D.; Groves, J. T. *J. Inorg. Biochem.* **2007,** *101*, 1786–1797. (b) Jin, N.; Groves, J. T. *J. Am. Chem. Soc.* **1999,** *121*, 2923–2924. (c) Lee, R. W.; Nakagaki, P. C.; Bruice, T. C. *J. Am. Chem. Soc.* **1989,** *111*, 1368–1372. (d) Bernadou, J.; Fabiano, A.-S.; Robert, A.; Meunier, B. *J. Am. Chem. Soc.* **1994,** *116*, 9375–9376.

(12) Zhang, R.; Newcomb, M. *Acc. Chem. Res.* **2008,** *41*, 468–477.

(13) Fukuzumi, S.; Fujioka, N.; Kotani, H.; Ohkubo, K.; Lee, Y.-M.; Nam, W. *J. Am. Chem. Soc.* **2009,** *131*, 17127–17134.

(14) (a) Gross, Z.; Golubkov, G.; Simkhovich, L. *Angew. Chem., Int. Ed.* **2000,** *39*, 4045–4047. (b) Liu, H.-Y.; Lai, T.-S.; Yeung, L.-L.; Chang, C. K. *Org. Lett.* **2003,** *5*, 617–620. (c) Liu, H.-Y.; Yan, F.; Xie, Y.-T.; Li, X.-Y.; Chang, C. K. *J. Am. Chem. Soc.* **2009,** *131*, 12890–12891.

(15) (a) Zhang, R.; Harischandra, D. N.; Newcomb, M. *Chem.—Eur. J.* **2005,** *11*, 5713–5720. (b) Gao, Y.; Åkermark, T.; Liu, J.; Sun, L.; Åkermark, B. *J. Am. Chem. Soc.* **2009,** *131*, 8726–8727.

(16) (a) Ramdhanie, B.; Stern, C. L.; Goldberg, D. P. *J. Am. Chem. Soc.* **2001,** *123*, 9447–9448. (b) Mandimutsira, B. S.; Ramdhanie, B.; Todd, R. C.; Wang, H. L.; Zareba, A. A.; Czernuszewicz, R. S.; Goldberg, D. P. *J. Am. Chem. Soc.* **2002,** *124*, 15170–15171.

(17) (a) Lansky, D. E.; Mandimutsira, B.; Ramdhanie, B.; Clausén, M.; Penner-Hahn, J.; Zvyagin, S. A.; Telser, J.; Krzystek, J.; Zhan, R. Q.; Ou, Z. P.; Kadish, K. M.; Zakharov, L.; Rheingold, A. L.; Goldberg, D. P. *Inorg. Chem.* **2005,** *44*, 4485–4498. (b) Kerber, W. D.; Goldberg, D. P. *J. Inorg. Biochem.* **2006,** *100*, 838–857.

(18) (a) Goldsmith, C. R.; Cole, A. P.; Stack, T. D. P. *J. Am. Chem. Soc.* **2005,** *127*, 9904–9912. (b) Parsell, T. H.; Yang, M.-Y.; Borovik, A. S. *J. Am. Chem. Soc.* **2009,** *131*, 2762–2763. (c) Gunay, A.; Theopold, K. H. *Chem. Rev.* **2010,** *110*, 1060–1081. (d) Yin, G. C.; Danby, A. M.; Kitko, D.; Carter, J. D.; Scheper, W. M.; Busch, D. H. *J. Am. Chem. Soc.* **2007,** *129*, 1512–1513. (e) Kurahashi, T.; Kikuchi, A.; Shiro, Y.; Hada, M.; Fujii, H. *Inorg. Chem.* **2010,** *49*, 6664–6672. (f) Reece, S. Y.; Nocera, D. G. *Annu. Rev. Biochem.* **2009,** *78*, 673–699. (g) Nieto, I.; Ding, F.; Bontchev, R. P.; Wang, H.; Smith, J. M. *J. Am. Chem. Soc.* **2008,** *130*, 2716–2717. (h) Mayer, J. M. *Annu. Rev. Phys. Chem.* **2004,** *55*, 363–390. (i) Mayer, J. M.; Mader, E. A.; Roth, J. P.; Bryant, J. R.; Matsuo, T.; Dehestani, A.; Bales, B. C.; Watson, E. J.; Osako, T.; Valiant-Saunders, K.; Lam, W. H.; Hrovat, D. A.; Borden, W. T.; Davidson, E. R. *J. Mol. Catal. A: Chem.* **2006,** *251*, 24–33.

(19) (a) Goldberg, D. P. *Acc. Chem. Res.* **2007,** *40*, 626–634. (b) Lansky, D. E.; Goldberg, D. P. *Inorg. Chem.* **2006,** *45*, 5119–5125. (c) Prokop, K. A.; de Visser, S. P.; Goldberg, D. P. *Angew. Chem., Int. Ed.* **2010,** *49*, 5091–5095.

(20) (a) Marcus, R. A. *Annu. Rev. Phys. Chem.* **1964,** *15*, 155–196. (b) Marcus, R. A. *Angew. Chem., Int. Ed. Engl.* **1993,** *32*, 1111–1121.

(21) (a) Fukuzumi, S.; Ohkubo, K.; Tokuda, Y.; Suenobu, T. *J. Am. Chem. Soc.* **2000,** *122*, 4286–4294. (b) Fukuzumi, S.; Koumitsu, S.; Hironaka, K.; Tanaka, T. *J. Am. Chem. Soc.* **1987,** *109*, 305–316.

(22) Armarego, W. L. F.; Chai, C. L. L. *Purification of Laboratory Chemicals*, 5th ed.; Butterworth Heinemann: Amsterdam, 2003.

(23) Fukuzumi, S.; Tokuda, Y.; Kitano, T.; Okamoto, T.; Otera, J. *J. Am. Chem. Soc.* **1993,** *115*, 8960–8968.

(24) (a) Anderson, A. G., Jr.; Berkelhammer, G. *J. Am. Chem. Soc.* **1958,** *80*, 992–999. (b) Mauzerall, D.; Westheimer, F. H. *J. Am. Chem. Soc.* **1955,** *77*, 2261–2264. (c) Caughey, W.; Schellenberg, K. A. *J. Org. Chem.* **1966,** *31*, 1978–1982.

(25) (a) Zdilla, M. J.; Dexheimer, J. L.; Abu-Omar, M. M. *J. Am. Chem. Soc.* **2007,** *129*, 11505–11511. (b) Camenzind, M. J.; Hollander, F. J.; Hill, C. L. *Inorg. Chem.* **1983,** *22*, 3776–3784. (c) Guilard, R.; Perié, K.; Barbe, J.-M.; Nurco, D. J.; Smith, K. M.; Caemelbecke, E. V.; Kadish, K. M. *Inorg. Chem.* **1998,** *37*, 973–981.

(26) Banci, L.; Bencini, A.; Benelli, C.; Gatteschi, D.; Zanchini, C. *Struct. Bonding* **1982,** *52*, 37–86.

(27) Parsell, T. H.; Behan, R. K.; Green, M. T.; Hendrick, M. P.; Borovik, A. S. *J. Am. Chem. Soc.* **2006,** *128*, 8728–8729.

(28) (a) Krzystek, J.; Ozarowski, A.; Telser, J. *Coord. Chem. Rev.* **2006,** *250*, 2308–2324. (b) Duboc, C.; Collomb, M. *Chem. Commun.* **2009,** 2715–2717.

(29) Mann, C. K.; Barnes, K. K. *Electrochemical Reactions in Nonaqueous Systems*; Marcel Dekker: New York, 1970.

(30) (a) Lee, Y.-M.; Kotani, H.; Suenobu, T.; Nam, W.; Fukuzumi, S. *J. Am. Chem. Soc.* **2008,** *130*, 434–435. (b) Comba, P.; Fukuzumi, S.; Kotani, H.; Wunderlich, S. *Angew. Chem., Int. Ed.* **2010,** *49*, 2622–2625. (c) Fukuzumi, S.; Kotani, H.; Suenobu, T.; Hong, S.; Lee, Y.-M.; Wonwoo, N. *Chem.—Eur. J.* **2010,** *16*, 354–361.

(31) Yang, E. S.; Chan, M.-S.; Wahl, A. C. *J. Phys. Chem.* **1980,** *84*, 3094–3099.

(32) The relevant pK_a values in DMSO have been reported to be pK_a(CH_3CO_2H) = 12.3, pK_a(CF_3CH_2OH) = 23.5, and pK_a-(CH_3OH) = 29.0. See: Bordwell, F. G. *Acc. Chem. Res.* **1988,** *21*, 456–463.

(33) Huynh, M. H. V.; Meyer, T. J. *Chem. Rev.* **2007,** *107*, 5004–5064.

(34) Fukuzumi, S. *Prog. Inorg. Chem.* **2009,** *56*, 49–153.

(35) (a) Yuasa, J.; Yamada, S.; Fukuzumi, S. *J. Am. Chem. Soc.* **2006,** *128*, 14938–14948. (b) Miyazaki, S.; Kojima, T.; Mayer, J. M.; Fukuzumi, S. *J. Am. Chem. Soc.* **2009,** *131*, 11615–11624. (c) Matsuo, T.; Mayer, J. M. *Inorg. Chem.* **2005,** *44*, 2150–2158.

(36) (a) He, G.-X.; Blasko, A.; Bruice, T. C. *Bioorg. Chem.* **1993,** *21*, 423–430. (b) Ohno, A. *J. Phys. Org. Chem.* **1995,** *8*, 567–576.

(37) (a) Fukuzumi, S.; Kotani, H.; Lee, Y.-M.; Nam, W. *J. Am. Chem. Soc.* **2008,** *130*, 15134–15142. (b) Jeong, Y. J.; Kang, Y.; Han, A.-R.; Lee, Y.-M.; Kotani, H.; Fukuzumi, S.; Nam, W. *Angew. Chem., Int. Ed.* **2008,** *47*, 7321–7324.

(38) (a) Fukuzumi, S.; Nishizawa, N.; Tanaka, T. *J. Org. Chem.* **1984,** *49*, 3571–3578. (b) Fukuzumi, S.; Nishizawa, N.; Tanaka, T. *J. Chem. Soc., Perkin Trans. 2* **1985,** 371–378.

■ NOTE ADDED AFTER ASAP PUBLICATION

There was a change in a compound name in the abstract in the version reposted January 20, 2011.